Biochimica et Biophysica Acta 1850 (2015) 1169–1179

Contents lists available at ScienceDirect

Biochimica et Biophysica Acta

journal homepage: www.elsevier.com/locate/bbagen

Anti-angiogenic activities of snake venom CRISP isolated from *Echis carinatus sochureki*

Shimon Lecht [a], Rachel A. Chiaverelli [a], Jonathan Gerstenhaber [a], Juan J. Calvete [b], Philip Lazarovici [c], Nicholas R. Casewell [d], Robert Harrison [d], Peter I. Lelkes [a], Cezary Marcinkiewicz [a,*]

[a] Temple University, College of Engineering, Department of Bioengineering, Philadelphia, PA, USA
[b] Instituto de Biomedicina de Valencia, Consejo Superior de Investigaciones Cientificas, 46010 Valencia, Spain
[c] The Hebrew University of Jerusalem, School of Pharmacy, Institute for Drug Research, Jerusalem, Israel
[d] The Alistar Reid Venom Research Unit, Liverpool School of Tropical Medicine, Liverpool L3 5QA, United Kingdom

ARTICLE INFO

Article history:
Received 1 October 2014
Received in revised form 20 January 2015
Accepted 1 February 2015
Available online 7 February 2015

Keywords:
Angiogenesis
CRISP
Endothelial cells
Cell proliferation
Migration

ABSTRACT

Background: Cysteine-rich secretory protein (CRISP) is present in majority of vertebrate including human. The physiological role of this protein is not characterized. We report that a CRISP isolated from *Echis carinatus sochureki* venom (ES-CRISP) inhibits angiogenesis.
Methods: The anti-angiogenic activity of purified ES-CRISP from snake venom was investigated *in vitro* using endothelial cells assays such as proliferation, migration and tube formation in Matrigel, as well as *in vivo* in quail embryonic CAM system. The modulatory effect of ES-CRISP on the expression of major angiogenesis factors and activation of angiogenesis pathways was tested by qRT-PCR and Western blot.
Results: The amino acid sequence of ES-CRISP was found highly similar to other members of this snake venom protein family, and shares over 50% identity with human CRISP-3. ES-CRISP supported adhesion to endothelial cells, although it was also internalized into the cytoplasm in a granule-like manner. It blocked EC proliferation, migration and tube formation in Matrigel. In the embryonic quail CAM system, ES-CRISP abolished neovascularization process induced by exogenous growth factors (bFGF, vpVEGF) and by developing gliomas. CRISP modulates the expression of several factors at the mRNA level, which were characterized as regulators of angiogenesis and blocked activation of MAPK Erk1/2 induced by VEGF.
Conclusions: ES-CRISP was characterized as a negative regulator of the angiogenesis, by direct interaction with endothelial cells.
General significance: The presented work may lead to the development of novel angiostatic therapy, as well as contribute to the identification of the physiological relevance of this functionally uncharacterized protein.

1. Introduction

Angiogenesis is one of the key processes involved in remodeling of the tissue microenvironment that leads to the progression of solid cancers. Since the first observations of pathological vessel growth by Judah Folkman [1], a large number of studies have been performed to investigate tumor neovascularization. Many endogenous modulators of angiogenesis have been identified, and the list of new members is still growing [2]. Cancer progression is determined by the balance between stimulators and inhibitors of angiogenesis. Thus, overexpression of pro-angiogenic factors leads to cancer development beyond the initial size (approximately 1–2 mm^3) by 'turning on' the 'angiogenic switch' for pathological vessel growth [3]. Growth factors, such as VEGF, bFGF, PDGF and TGF-α/β are important angiogenesis stimulators. Other positive regulators of this process belong to the families of cytokines or oncogenes. Endogenous angiogenesis inhibitors comprise physiologically cleaved fragments of ECM proteins (angiostatin, endostatin), interferons, PF4, TIMPs and many others. Understanding the mechanisms responsible for destabilizing the balance of angiogenesis modulators may offer new opportunities for designing novel, more effective cancer therapies. Currently, available cancer angiogenic therapy is based on the immune-blocking of VEGF [4].

Snake venoms represent a rich source of biological active molecules, which have been intensively used as pharmacological tools for drug discovery or for studying biological processes such as angiogenesis. The best studied venom compounds affecting neovascularization are

Abbreviations: ES-CRISP, *Echis carinatus sochureki* cysteine-rich secretory protein; CMFDA, 5-chloromethylfluororescein diacetate; CAM, chorioallantoic membrane; EC, endothelial cell; gHMVEC, glioma human microvascular endothelial cells; HUVEC, human umbilical cord endothelial cells; HAEC, human aortic endothelial cells; D_f, fractal dimension; bFGF, basic fibroblast growth factor; vpVEGF, *Vipera palestinae* vascular endothelial growth factor; hrVEGF, human recombinant VEGF; TSP-1, thrombospondin-1; FAK, focal adhesion kinase; MAPK, mitogen-activated protein kinase

* Corresponding author at: Temple University, CoE, Department of Bioengineering, 1947 N.12th St., Philadelphia, PA 19122, USA. Tel.: +1 215 204 3301; fax: +1 215 204.
E-mail address: cmarcink@temple.edu (C. Marcinkiewicz).

http://dx.doi.org/10.1016/j.bbagen.2015.02.002
0304-4165/

proteins, which interact with integrins expressed on endothelial cells. These proteins serve mainly as inhibitors of angiogenesis and are members of the disintegrins family [5,6]. The most potent anti-angiogenic effect is typically attributed to disintegrins that contain an RGD motif in their active sites. These disintegrins target αvβ3 integrin and act by blocking the pro-angiogenic activities of endothelial cells, such as proliferation and migration, and in certain cases inducing apoptosis. Some of the non-RGD-containing disintegrins that are also inhibitors of angiogenesis express biologically MLD and KTS active motifs and block α9β1 and α1β1 integrins, respectively [7]. C-type lectins (CLPs) are another group of snake venom proteins regulate angiogenesis by binding to integrin receptors [8,9]. Snake venom phospholipases A2 are reportedly angiostatic compounds, as they bind to the RGD-dependent integrins on endothelial cells in a non-enzymatic manner [10]. In this paper we report that snake venom cysteine-rich secretory protein (CRISP) is also an anti-angiogenic protein that acts through interactions with endothelial cells.

CRISPs are found in the majority of snake venoms [11,12]. The structure of the venom CRISPs has been established by X-ray crystallography [13,14]. CRISPs are single polypeptide molecules containing 16 cysteines, which are involved in internal linkage through disulfide bonds. The modeled 3-D structure revealed the presence of two domains: N-terminal globular domain and C-terminal cysteine-rich domain. The cysteine-rich domain contains two Zn^{2+}-binding motifs, which the functional roles remain unclear [15]. The biological activity of snake venom CRISPs is still not fully understood; some were characterized as blockers of L-type calcium channels [16] and cyclic nucleotide gated channels [17]. Although *ex vivo*, CRISPs block rat arterial smooth muscle contraction [16], they appear to belong to the non-toxic components of snake venoms, because they have no toxic effects on mice or insect [18]. Recent studies showed that CRISP isolated from cobra venom, activates endothelial cells as inferred from the increased expression adhesion molecules (VCAM-1 and ICAM-1) and E-selectin [19].

CRISP proteins are expressed in a wide variety of organisms, including human. Thus, the human CRISP-3 (SGP28) exhibits strong structural similarity to snake venom CRISP. CRISP-3 is found in human saliva, seminal plasma, sweat and in blood plasma at a relatively high level of 6.3 μg/ml [20]. This protein is produced by immune cells such as B lymphocytes, neutrophils, and eosinophils, suggesting that it may be a part of the innate immune system. CRISP-3 was characterized as forming a complex with α1B-glycoprotein in blood plasma [21], and with prostate secretory protein of 94 (PSP94) in human seminal plasma [22]. Up-regulation of CRISP-3 expression was observed for tumoral tissue in prostate cancer patients [23], while it is down-regulated in oral tongue squamous cell carcinoma [24]. The role of CRISP-3 in cancer pathology remains unknown. Here we present data suggesting that CRISP-3 may be an endogenous regulator of cancer-related angiogenesis.

2. Materials and methods

2.1. Snake venom proteins, antibodies and other reagents

ES-CRISP, echistatin (a disintegrin) and sochicetin-A (CLP) were purified from *Echis carinatus sochureki* venom (Latoxan Serpentarium, Valence, France) by sequential fractionation on gel filtration, cation-exchange and RP-HPLC columns as described previously [25]. Briefly, crude venom was applied to a size exclusion Superdex 200 column (2 × 100 cm) and fractionated into six major fractions. Fraction I, was applied to a reverse-phase HPLC (RP-HPLC) C_{18} column (25 × 1 cm) at a flow rate 2 ml/ml with a linear acetonitrile gradient 0–80% in 0.1% TFA over 45 min. Pure sochicetin-A was collected as fraction 2. Echistatin and ES-CRISP were purified from gel filtration fraction IV, which was applied to a MonoS column. Proteins that were not retained on the column were separated by RP-HPLC as above. Pure echistatin was collected as fraction 2, whereas pure ES-CRISP was collected as fraction 10 (Fig. 1A).

Ethylpyridylation (EP) of ES-CRISP for structural analysis was performed according to the procedure described earlier for snake venom disintegrins [26]. Isolated subunits were analyzed by N-terminal sequencing using an Applied Biosystems 477A instrument. Molecular masses of sochicetins and their subunits were evaluated by SDS-PAGE and confirmed by MALDI-TOF. The amino acid sequence of ES-CRISP was established based on the transcriptome of *E.c. sochureki* as described previously [27].

Labeling of ES-CRISP with FITC was performed according to the protocol described earlier for snake venom disintegrins [28].

Polyclonal antibodies against human CRISP-3 and β-actin developed in goat, and anti-β1 integrin subunit developed in rabbit were purchased from Santa Cruz Biotech (Dallas, TX). A monoclonal antibody against TSP-1 (clone 2D11) was kindly provided by Dr. David Roberts (National Cancer Institute, NIH, Bethesda, MD). Antibodies against all cell signaling molecules (phosphorylated and total) were purchased from Cell Signaling Techn. (Danvers, MA). Fibronectin and vitronectin isolated from human plasma were purchased from Millipore Inc (Billerica, MA); equine tendon collagen I was purchased from Chrono-Log Corp. (Haverton, PA); and laminin was purchased from Engelbreth-Holm-Swarm murine sarcoma basement membrane from Sigma Inc. (St. Louis, MI). vpVEGF was purified from *Vipera palestinae* venom according to the procedure described earlier [29]; bFGF was purchased from Sigma Inc.

2.2. Cell culture

Primary endothelial cells were used throughout passages 2 to 6. Glioma-derived human microvascular endothelial cells (gHMVEC) were isolated from tumor tissue obtained from patients undergoing standard surgical procedure for diagnosed glioblastoma multiform as described earlier [30]. Human umbilical vein endothelial cells (HUVEC) and human aortic endothelial cells (HAEC) were purchased from Lonza Inc (Lonza Walkerscille, Inc., Walkersville, MD). Cells were cultured in the presence of complete endothelial cell basal media-2 (Lonza Inc.) at 37 °C and 5% CO_2 atmosphere.

Human cancer cell lines used for the cell adhesion experiment were purchased from ATCC (Manassas, VA), except for the human melanoma cell line, which was kindly provided by Dr. E. Danen (Leiden University, Leiden, The Netherlands). All cell lines were cultured in DMEM (Invitrogen, Carlsbad, CA), containing 10% FBS at 37 °C and 5% CO_2 atmosphere.

2.3. Cell adhesion assay

Cell adhesion was performed using CellTracker™ green CMFDA (5-chloromethylfluororescein diacetate)-labeled cell as described previously [28]. Briefly, snake venom proteins, or ECM proteins were immobilized on the 96-well plate in PBS overnight at 4 °C. The plate was blocked with 1% BSA in Hank's balanced salt solution (HBSS) containing 5 mM $MgCl_2$. Cells were labeled with 12.5 μM CMFDA and plated (1×10^5 per sample) into the wells in the presence or absence of sochicetins. Plates were incubated at 37 °C for 60 min. Thereafter, unbound cells were removed by washing and bound cells lysed with 0.5% Triton X-100. A standard curve was prepared in parallel on the same plates using known concentrations of labeled cells. The plates were read using fluorescence a plate reader (Bio-Tek) with 485 nm excitation and 530 nm emission filters.

2.4. Immunocytochemistry

Glass tissue culture chamber slides (4-well) were coated with ES-CRISP, echistatin or fibronectin in concentration 10 μg/ml at 4 °C. Slides were blocked with 1% BSA in DMEM, then cells (2×10^4/ml) were added

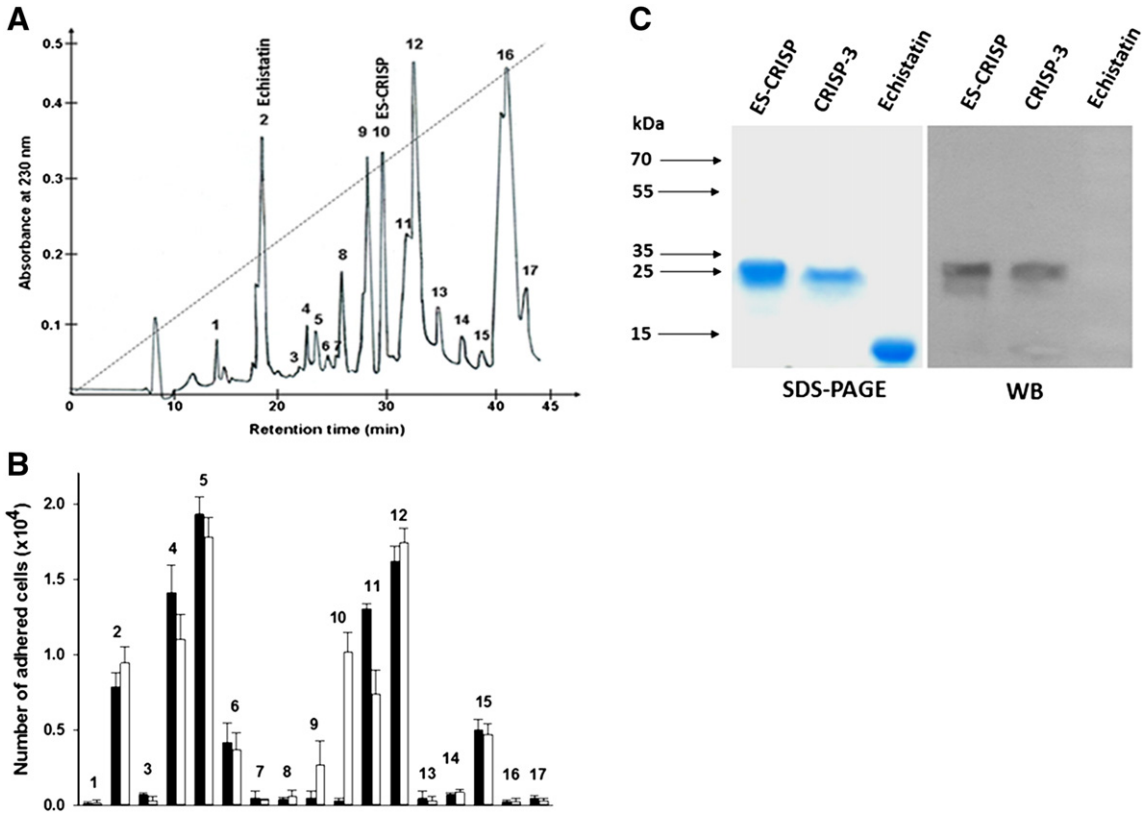

Fig. 1. Purification and identification of ES-CRIS. (A) Separation profile of ECIV(1) fraction on HPLC-RP. ECIV(1) fraction obtained from the crude snake venom through gel filtration and ion exchange chromatography, was applied on C_{18} column and elution was performed with linear gradient (dashed lines) of increased concentration of acetonitrile (0–80%) in 0.1% TFA. Fractions were collected manually and lyophilized. Fractions containing echistatin and ES-CRISP are indicated. (B) Adhesion of LN18 cell line and HUVEC to immobilized proteins obtained from RP-HPLC separation of ECIV(1) fraction. Proteins (20 μg/ml) were immobilized on 96-well plate by overnight incubation at 4 °C. Adhesion of CMFDA-labeled LN18 cells (filled bars) and HUVEC (open bars) was calculated from standard curve of known number of cells reflecting intensity of fluorescence. Error bars represent S.D. from three independent experiments. (C) SDS-PAGE (left panel) and Western blot (right panel) analysis of purified ES-CRISP. Proteins (10 μg for SDS-PAGE and 2 μg for WB) were applied on 12.5% gel in reducing conditions. WB was performed using goat anti-human CRISP-3 polyclonal antibody.

to the chambers and incubated for 60 min at 37 °C. Cells were fixed with 4% paraformaldehyde, washed with PBS and observed by phase-contrast microscopy (Olympus IX81; 160× magnification). For analyzing cell spreading, fixed cells were permeabilized for 5 min on ice with 0.2% Triton X-100 in PBS, and TRITC-phalloidin (Millipore Inc.) added to visualize F-actin. Nuclei were visualized by DAPI present in the slide mounting buffer (Vector Labs., Burlingame, CA). Cell images were captured by fluorescence microscopy at 400× magnification. The areas single spread cells were calculated using MetaMorph software for thresholded images. Statistical evaluation was based on calculation of at least 50 cells per group.

For confocal microscope imaging, cells were cultured on the chamber slides to 90% confluence, and incubated with FITC-ES-CRISP (20 μg/ml) at 37 °C for 60 min. After fixation with 2% paraformaldehyde and permeabilization with 0.2% Triton X-100, cells were stained with TRITC-phalloidin and mounted in buffer containing DAPI. Images were collected using confocal laser scanning microscope (Olympus IX83), with 60× oil objective.

2.5. Flow cytometry

HUVEC were re-suspended in HBSS containing calcium and magnesium, and 1% BSA (5×10^5 per 200 μl) and incubated with increasing doses of FITC-ES-CRISP for 30 min at 37 °C. Thereafter, the cells were fixed by adding 100 μl of 4% paraformaldehyde. The binding of FITC-ES-CRISP to HUVEC was analyzed using an Accuri C6 flow cytometer (BD Bioscience, San Jose, CA). Unlabeled cells, subjected to the same procedure, were used as negative control.

2.6. Cell proliferation

Cells were grown to 60–70% of confluence in 24-well plates and starved for 24 h. 2% FBS was added in DMEM supplemented (or not) with different CRISP concentrations to test inhibitory effects. Cells were fixed every 24 h, stained with DAPI and the nuclei of viable cells counted manually at 100× magnification in a fluorescence microscopy. Error bars represent S.D. from triplicated experiments, counted from at least five different observation fields per well.

Alternatively, cell proliferation was measured by incorporation of a BrdUrd, using commercially available kit (Roche, Mannheim, Germany) as described previously [31].

2.7. Cell migration

Cell migration in Boyden chambers (chemotaxis) was performed using 8 μm pore size membrane inserts (HTS FluoroBlok inserts, BD Biosciences), as described previously [31].

Wound healing was studied in 24 well plates. Fully confluent cell layers were scratched with 200 μl pipette tips to generate artificial wounds in the monolayers. 2% FBS was used for stimulation of cell migration in the presence or absence of different concentrations of ES-CRISP. Plates were incubated at 37 °C in 5% CO_2 atmosphere for 24 h. The extent of wound closure was calculated based on the estimated width of the scratch at the beginning and end of experiment using an Olympus IX81 microscope imagining system with MetaMorph software.

2.8. Western blotting

Western blotting analysis was performed as described earlier [31]. Briefly, SDS-PAGE was performed using precast 10% gel (BioRad Inc.). Cells were lysed in the presence of proteases and phosphatases inhibitors, lysates (20 μg protein) were loaded on the gel and electrophoresis was performed in reduced conditions. Gel was blotted into PVDF membrane, which was blocked by 5% milk and exposed to the appropriate primary and HRP-conjugated secondary antibody for chemiluminescent detection. Blot was imaged using C-DiGit Blot Scanner (LI-COR Inc.).

2.9. Endothelial tube formation in Matrigel

The Matrigel tube formation assay, an *in vitro* model of angiogenesis, was performed as described previously [30]. Briefly, growth factor-reduced Matrigel (BD Biosciences) was plated onto 24-well plates and incubated at 37 °C for 30 min. HUVEC were seeded at 5×10^4/well in EBM-2 containing 2% FBS, as an angiogenesis inducer, in the presence or absence of snake venom proteins. After 24 h the medium was removed, and the cells were washed twice with PBS and fixed with 4% paraformaldehyde. Phase-contrast images were analyzed in an Olympus IX81 microscope with 100× magnification. The numbers of branching points per observation field were determined and averaged for each well.

2.10. Angiogenesis in embryonic quail CAM system

The quail embryonic model of angiogenesis was used to detect angiostatic activities of ES-CRISP, as described previously [30]. Pathological angiogenesis was induced by treatment with pro-angiogenic growth factors (vpVEGF and bFGF), or progressing glioma after implantation of the LN18 or LN229 cell lines onto the quail chorioallantoic membrane (CAM).

2.11. qRT-PCR array analysis

The effects of ES-CRISP on the gene expression of major angiogenesis factors in HUVEC were investigated using The Human Angiogenesis RT^2 Profiler PCR Array (from SABiosciences/Qiagen Inc., Germantown, MD), as described previously [32]. Briefly, the 96-well PCR array plate contained 84 angiogenesis-focused human genes, 5 housekeeping genes, a genomic DNA control, 3 RT controls and 3 positive PCR controls. HUVEC were treated with ES-CRISP (20 μg/ml) for 24 h at 37 °C. Total RNA was isolated using RNeasy mini kits (Qiagen) and cDNAs were reverse transcribed using the RT^2 PCR array first strand kit (Qiagen). PCR was performed using the RT^2 SYBR Green qPCR Mastermix (Qiagen) in an Eppendorf Mastercycler (Ep Realplex II). Data were analyzed using the $2^{-\Delta\Delta Ct}$ method.

2.12. Statistical analysis

Statistical analysis was performed by Student's *t*-test or by one-way ANOVA of variance followed by the Dunnett's test for multiple comparisons, where appropriate. Calculations were carried out using SigmaPlot 12 (SPSS Inc., Chicago, IL).

3. Results

3.1. Purification and structural analysis of ES-CRISP

E.c. sochureki venom was chromatographically fractionated by RP-HPLC from sub-fraction ECIV(1), obtained as described previously [25] (Fig. 1A). The fractions were screened for interaction with glioma cell line LN18 and primary HUVEC in a cell adhesion assay. A number of fractions, supported adhesion of the glioma cells and of HUVEC (Fig. 1B). However, fractions 9 and 10 showed diversity to bind both cell types, because they did not interact with cancer cells but showed pro-adhesive properties for ECs. Fraction 10 was identified as ES-CRISP and its purity was verified by SDS-PAGE (Fig. 1C) and by MALDI-TOF. Mass spectroscopy analysis revealed the molecular mass of ES-CRISP to be 24,462 Da and its comparison with the ethylpyridylated (EP) form indicated the presence of 16 cysteines in the single polypeptide chain. The EP-protein was N-terminal sequenced to reveal that the first 15 amino acids matched the sequence of other snake venom CRISPs, with a near 100% similarity (Fig. 2). Moreover, the anti-human CRISP-3 antibody showed significant cross-reactivity to ES-CRISP in

```
ES-CRISP          NVDFDSESPRKPEIQNEIIDLHNSLRRSVNPTASNMLKMEWYPEAAANAERWAFQ
VB-CRISP          NVDFDSESPRKPEIQNEIIDLHNSLRRSVNPTASNMLKMEWYPEAAANAERWAFR
Triflin           NVDFDSESPRKPEIQNEIIDLHNSLRRSVNPTASNMLKMEWYPEAAANAERWAYR
Natrin            NVDFNSESTRRKKKQKEIVDLHNSLRRRVSPTASNMLKMEWYPEAADNAERWANT
CRISP-3     ANEDKDPAFTALLTTQTQVQREIVNKHNELRRAVSPPARNMLKMEWNKEAAANAQKWANQ

ES-CRISP    CILDHSPRESRVINGIKCGENIYMSSVPKLWTAIIHKWHDEKKNFVYGIGASPSNAVTGH
VB-CRISP    CILSHSPRDSRVIGGIKCGENIYMSTSPMKWTAIIHEWHGEEKDFVYGQGASPANAVVGH
Triflin     CIESHSSRDSRVIGGIKCGENIYMATYPAKWTDIIHAWHGEYKDFKYGVGAVPSDAVIGH
Natrin      CSLNHSPDNLRVLEGIKCGENIYMSSNARTWTEIIHLWHDEYKNFVYGVGANPPGSVTGH
CRISP-3     CNYRHSNPKDRMTSL-KCGENLYMSSASSSWSQAIQSWFDEYNDFDFGVGPKTPNAVVGH

ES-CRISP    YTQIVWYKSHRGGCAAAYCPSSEYN-YFYVCQYCPTGNIIGKTATPYTSGPPCGECPSAC
VB-CRISP    YTQIVWYKSYRSGCAAAYCPSSEYK-YFYVCQYCPAGNMQGKTATPYTSGPPCGDCPSAC
Triflin     YTQIVWYKSYRAGCAAAYCPSSKYS-YFYVCQYCPAGNIIGKTATPYKSGPPCGDCPSDC
Natrin      YTQIVWYQTYRAGCAVSYCPSSAWS-YFYVCQYCPSGNFQGKTATPYKLGPPCGDCPSAC
CRISP-3     YTQVVWYSSYLVGCGNAYCPNQKVLKYYYVCQYCPAGNWANRLYVPYEQGAPCASCPDNC

ES-CRISP    DNGLCTNPCTHRDEFTNCPDLVKQG-CQTKYLKSNCAASCFCHSEIK (220 aa)
VB-CRISP    DNGLCTNPCTHEDKFTNCKDLVKQG-CNNNYLKTNCPASCSCHNEII (220 aa)
Triflin     DNGLCTNPCTRENEFTNCDSLVQKSSCQDNYMKSKCPASCFCQNKII (221 aa)
Natrin      DNGLCTNPCTIYNKLTNCDSLLKQSSCQDDWIKSNCPASCFCRNKII (221 aa)
CRISP-3     DDGLCTNGCKYEDLYSNCKSLKLTLTCKHQLVRDSCKASCNCSNSIY (223 aa)
```

Fig. 2. Comparison of amino acid sequence of ES-CRISP polypeptide chain with CRISP molecules isolated from other snake venoms. Presented CRISP primary structure: VB-CRISP [12] from *Vipera berus*; Triflin [16] from *Trimeresurus flavoridis*; Natrin [14] from *Naja atra* and human CRISP-3 [44]. Cysteines are bold and underlined; identical amino acids in all molecules are highlighted in gray. Numbers of amino acids in polypeptide chains are indicated on the end. Dashes were applied to set up cysteines pattern.

contrast to echistatin, a monomeric, RGD-containing disintegrin isolated from the same venom (Fig. 1C). Echistatin was localized in fraction 2 of RP-HPLC separation (Fig. 1A).

The amino acid sequence of ES-CRISP was matched by CID-MS/MS to a single full-length transcript from the *E.c. sochureki* transcriptome, which showed very high level of amino acid sequence identity to other venom CRISPs and to human CRISP-3 (Fig. 2).

3.2. Interaction of ES-CRISP with endothelial cells

Purified ES-CRISP bound to distinct types of endothelial cells in a dose-dependent manner (Fig. 3A). The extent of ES-CRISP adhesion to ECs isolated from glioma (gHMVEC) was more pronounced than to HUVEC or HAEC. By contrast majority of tested cancer cell lines derived from different tumor tissues did not adhere to ES-CRISP with exception of only MV3 human melanoma cells (Fig. 3C). Interestingly, MV3 cells adhered to ES-CRISP to the same extent as HUVEC. On the other hand, the majority of cell types tested significantly adhered to echistatin.

We then tested the hypothesis that ES-CRISP might inhibit adhesion of ECs to various endogenous extracellular matrix (ECM) proteins. Surprisingly, we did not find any inhibitory effect on the adhesion of HUVEC to fibronectin, vitronectin, collagen type I and laminin (Fig. 3B). Integrin receptors antagonists identified and isolated from *E.c. sochureki* venom blocked integrin interaction with their respective ligands. For example, echistatin inhibited α5β1 integrin-dependent adhesion to fibronectin and αvβ3 integrin-dependent adhesion to vitronectin, whereas C-type lectin protein, sochicetin-A inhibited α2β1 integrin-dependent adhesion to collagen type I. None of the *E.c. sochureki* snake venom molecules blocked α6β1 integrin-dependent adhesion to laminin.

Endothelial cells exhibited differential spreading when seeded on ES-CRISP or the ECM protein, fibronectin. ES-CRISP-bound HUVEC remained rounded, whereas when seeded on echistatin, demonstrated limited spreading (Fig. 4A). Fully spread cell were observed after attachment to fibronectin. Moreover, fibronectin-bound cells exhibited well organized actin stress fibers, whereas cells adhered to the snake venom proteins showed atypical actin fiber organization (Fig. 4B).

Interestingly, ECs attached to echistatin expressed well-developed and condensed filopodia, in contrast to those attached to the ES-CRISP. This indicates that the mechanism of adhesion for echistatin is distinct

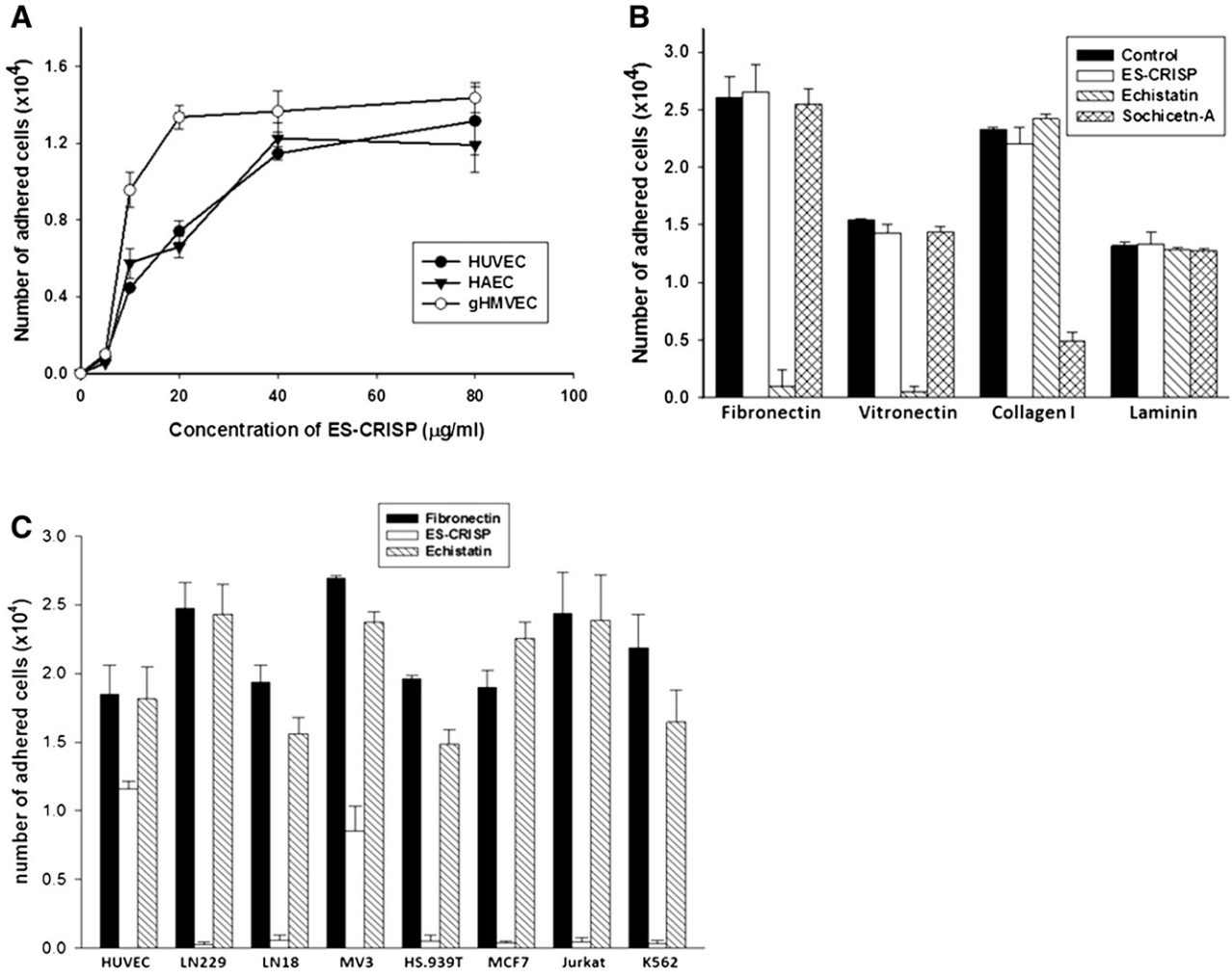

Fig. 3. Interaction of ES-CRISP with endothelial cells and various cancer cell lines in the cell adhesion assay. (A) Adhesion of three types of primary endothelial cells to immobilized different concentrations of ES-CRISP. (B) Effect of three proteins isolated from *E. c. sochureki* venom on the adhesion of HUVEC to different ECM proteins. ECM proteins were immobilized in amount of 10 μg/ml. Snake venom proteins were used at a concentration of 10 μg/ml. (C) Interaction of various cell types with ES-CRISP, echistatin and fibronectin in the cell adhesion assay. Snake venom and ECM proteins (10 μg/ml) were immobilized on a 96-well plate. Cancer cell lines: LN229 and LN18 developed from human glioblastoma; MV3 and HS.939T developed from human melanoma; MCF-7 developed from human breast tumor; and Jurkat and K562 developed from human lymphoma. Error bars for all experiments represent S.D. from three independent experiments.

from that for ES-CRISP and from endogenous ECM protein, fibronectin. Quantitative evaluation of the areas of three different types of ECs seeded on all three substrates confirmed lower values for snake venom molecules than for fibronectin (Fig. 4C). Interestingly, statistical evaluations showed significant differences not only for ES-CRISP and fibronectin, but also between both snake venom molecules calculated for all three cell types. ES-CRISP also potently bound to HUVEC in cell suspension. Flow cytometry analysis revealed FITC-labeled ES-CRISP binding to essentially 100% (99.1 ± 1.4) of the HUVEC population in a dose-dependent manner (Fig. 4D).

Confocal imaging of cultured HUVEC treated with FITC-labeled ES-CRISP revealed clusters of this protein on the cellular surface (top cell image) suggesting binding to a plasma membrane-anchored receptor (Fig. 4E). Significant amounts of protein were also internalized into the cytoplasm and appeared as endosome-like granules. Images taken from the plane of focus of 16 μm and 21 μm thicknesses of the cell clearly indicated spotty localization of clusters (green) of ES-CRISP in the vicinity of microfilaments (F-actin) visualized by phalloidin (red). The entire spectrum of the confocal planes of the cell displaying thickness of 24 μm and sectioned every 1.6 μm, is presented in Supplementary Fig. S1.

3.3. The effect of ES-CRISP on pro-angiogenic activities of cultured endothelial cells

We subsequently studied the effect of ES-CRISP on some of the pro-angiogenic activities of cultured ECs, such as cell proliferation (Fig. 5A), migration (Fig. 5B), and tubular morphogenesis in Matrigel (Fig. 5C). A BrdU incorporation-based assay revealed similar dose-dependent inhibition of proliferation by ES-CRISP in both HUVEC and microvascular EC isolated from human glioma (gHMVEC) (Fig. 5A, left panel). ES-CRISP also inhibited HUVEC proliferation measured over a period of 72 h by counting cell numbers (Fig. 5A, right panel). A statistically significant inhibition was observed for ES-CRISP concentrations exceeding 10 μg/ml. ES-CRISP potently blocked migration of HUVEC and gHMVEC in the wound healing and Boyden chamber chemotaxis assays (Fig. 5B). EC migration was inhibited in a dose-dependent manner in the artificial wound closure assay. Interestingly, cancer-derived EC were more resistant to ES-CRISP treatment in this assay then HUVEC, especially at lower doses. On the other hand, the extent of time-dependent inhibition of chemotaxis in the Boyden chamber was the same for both types of cells.

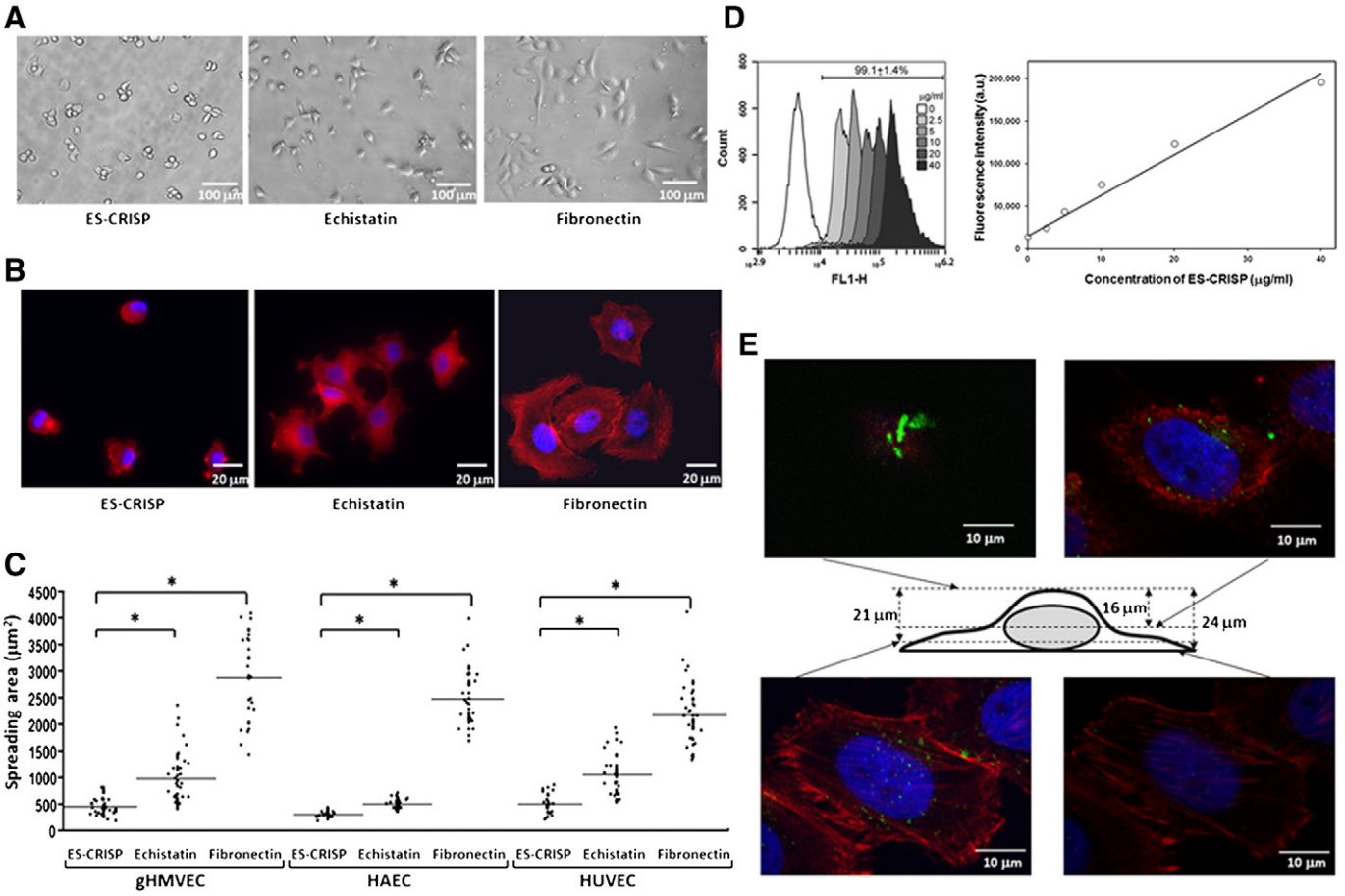

Fig. 4. Analysis of interaction of ES-CRISP with endothelial cells by microscopy and flow cytometry. (A) Morphology of HUVEC seeded on the different ligands. Glass slides were immobilized with snake venom proteins (20 μg/ml) or fibronectin (10 μg/ml) by overnight incubation at 4 °C. Cells (2×10^4/ml) were incubated on the slide by 60 min and fixed by 4% paraformaldehyde. Cells were analyzed by a phase-contrast microscope with 160× magnification. (B) Representative images of HUVEC cytoskeleton after cell adhesion and spreading on snake venom proteins and fibronectin. Cells were stained with TRITC-phalloidin for visualization of F-actin and DAPI to visualize nuclei. Cell images were captured using fluorescence microscope with 400× magnification. (C) Evaluation of spreading areas of three different types of endothelial cells. Adhered cells were stained with TRITC-phalloidin and spreading areas on the specific ligand were quantified. Data represent mean of >50. (*) $P < 0.001$ with ES-CRISP as a control. (D) Flow cytometry analysis of binding of FITC-labelled ES-CRISP to HUVEC. Cells (5×10^5 per sample) were incubated with different concentrations of FITC-ES-CRISP at 37 °C for 30 min. Cells were analyzed by flow cytometry. Histograms for increase concentrations of ES-CRISP are shown in the left panel; linear increasing of fluorescence intensity as a function of ES-CRISP is shown on the right panel. (E) Confocal images of HUVEC treated with FITC-ES-CRISP. Cells were cultured on the glass slides and treated with FITC-ES-CRISP (20 μg/ml) at 37 °C for 60 min. After fixation with 2% paraformaldehyde and permeabilization with 0.2% Triton X-100, cells were stained with TRITC-phalloidin and mounted by buffer containing DAPI. The images were taken from four different planes of focus, according to the specific cell thickness shown in diagram of cell presented in the center. 600× magnification with oil objective was applied in a scanning confocal microscope.

Capillary-like structure formation (tubular angiogenesis) in Matrigel is an established *in vitro* surrogate angiogenesis assay. ES-CRISP almost completely abolished tubular morphogenesis of HUVEC stimulated with 2% FBS (Fig. 5C). Interestingly, the number of branching points for ES-CRISP treated cells was even lower than that endogenously induced by growth-factor reduced Matrigel. Echistatin inhibited tube formation to

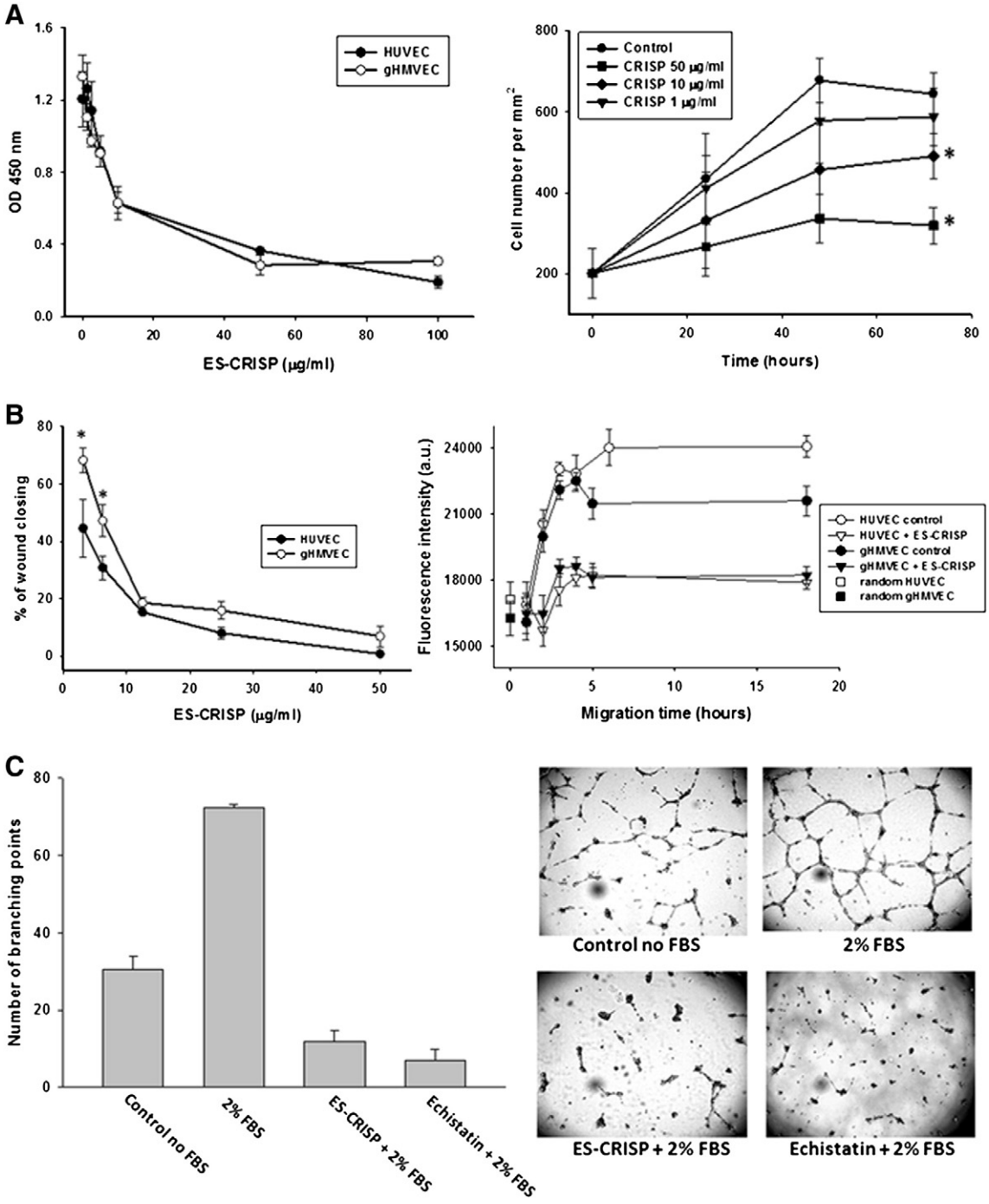

Fig. 5. Effect of ES-CRISP on pro-angiogenic activities of endothelial cells. (A) HUVEC proliferation assay measured by incorporation of BrdU (left panel), and viability assay measured by counting of viable cells (right panel). Cells (1×10^4) were grown on the 96-well plate up to 70% confluence and treated or not with different concentrations of ES-CRISP. 2% FBS was used for stimulation of cell proliferation. BrdUrd color development assay was performed according to the manufacturer's instruction (Roche). Cell viability assay was performed on the 24-well plate. HUVEC were fixed every 24 h, stained with DAPI and nuclei of viable cells were counted under a fluorescence microscope. Error bars represent S.D. from triplicated experiments. (*) significant difference in comparison to control ($P < 0.001$). (B) Wound healing assay (left panel) and chemotaxis assay in Boyden's chamber (right panel). Wound healing assay was initiated by scratching of 100% confluence HUVEC layer and was monitored after 24 h. Chemotaxis was performed in Boyden's chamber using 2% FBS as a chemoattractant. HUVEC were labeled with calcein, mixed with ES-CRISP (20 μg/ml) and applied on the top of fluoroblok membrane. Error bars represent S.D. from triplicate experiments. (*) significant difference between EC types ($P < 0.005$). (C) Tube formation assay of HUVEC in growth factor-reduced Matrigel. Cells were implemented into the Matrigel in the presence or absence of snake venom proteins (10 μg/ml). Graphic presentation of number of formed tubes (right panel) counted per microscopic observation field; representative images of Matrigel tubes (left panels). Error bars represent S.D. from counts performed by three different investigators on three separated experiments.

a similar extent as ES-CRISP, confirming previous reports that this snake venom disintegrin is a potent blocker of the pro-angiogenic activities of cultured EC [33].

3.4. Effect of ES-CRISP on angiogenesis in vivo

The anti-angiogenic activity of ES-CRISP was tested *in vivo* in the embryonic CAM assay (Fig. 6). ES-CRISP was a potent inhibitor of pathologically-induced angiogenesis when tested by exogenous application of growth factors or developing tumors. Stimulation of the CAM by bFGF or vpVEGF resulted in significant elevation of the vasculature ratio, which was reduced by ES-CRISP applied at doses of 20 μg and 40 μg to the level seen for control endogenous angiogenesis (Fig. 6A). ES-CRISP had a similar inhibitory effect on angiogenesis induced by implantation of the two glioma cell lines (LN18 and LN229) (Fig. 6B). This pathologically induced angiogenesis was completely reduced to the level of tumor-free membrane by ES-CRISP. Interestingly, treatment of the tumors with ES-CRISP also resulted in stabilization of microvasculature neighboring developing tumor (Supplementary Fig. S2).

3.5. Effect of ES-CRISP on the angiogenesis-regulating factors

Potential mechanisms involved in the inhibition of angiogenesis by ES-CRISP were investigated by the profiling of HUVEC for the gene expression of the major modulators of angiogenesis. Cells treated with ES-CRISP were analyzed using a focused RT-PCR microarray containing 84 key angiogenesis genes. Global analysis of the modulated genes indicated a differential pattern for the expression of these angiogenesis-related genes in ES-CRISP-treated cells and in control untreated cells (Supplementary Fig. S3). Furthermore, quantitative analysis of the gene expression revealed significant modulation by at least 2-fold for 18 genes that were down-regulated and 6 genes that were up-regulated (Table 1). These data suggest that ES-CRISP tilts the balance between pro- and anti-angiogenic genes towards an anti-angiogenic profile.

3.6. Effect of ES-CRISP on the modulation of pro-angiogenic signaling pathways in HUVEC

The effect of ES-CRISP was investigated on the modulation of major cellular signaling pathways, which are activated in endothelial cells in response to the VEGF treatment. ES-CRISP showed potent inhibitory effect on the phosphorylation of MAPK Erk1/2, whereas activation of two other MAP kinases, SAPK/JNK and p38, was not affected by this snake venom protein (Fig. 7A). No effect was also observed for the AKT activation, which is considered as a major pro-survival molecule involved in protection of cell against apoptosis (Fig. 7B).

Attachment and spreading of the cells induce focal adhesion. One of the major elements of this process is focal adhesion kinase (FAK), which undergoes autophosphorylation upon stimuli involving integrins. HUVEC following adhesion to the ES-CRISP showed no

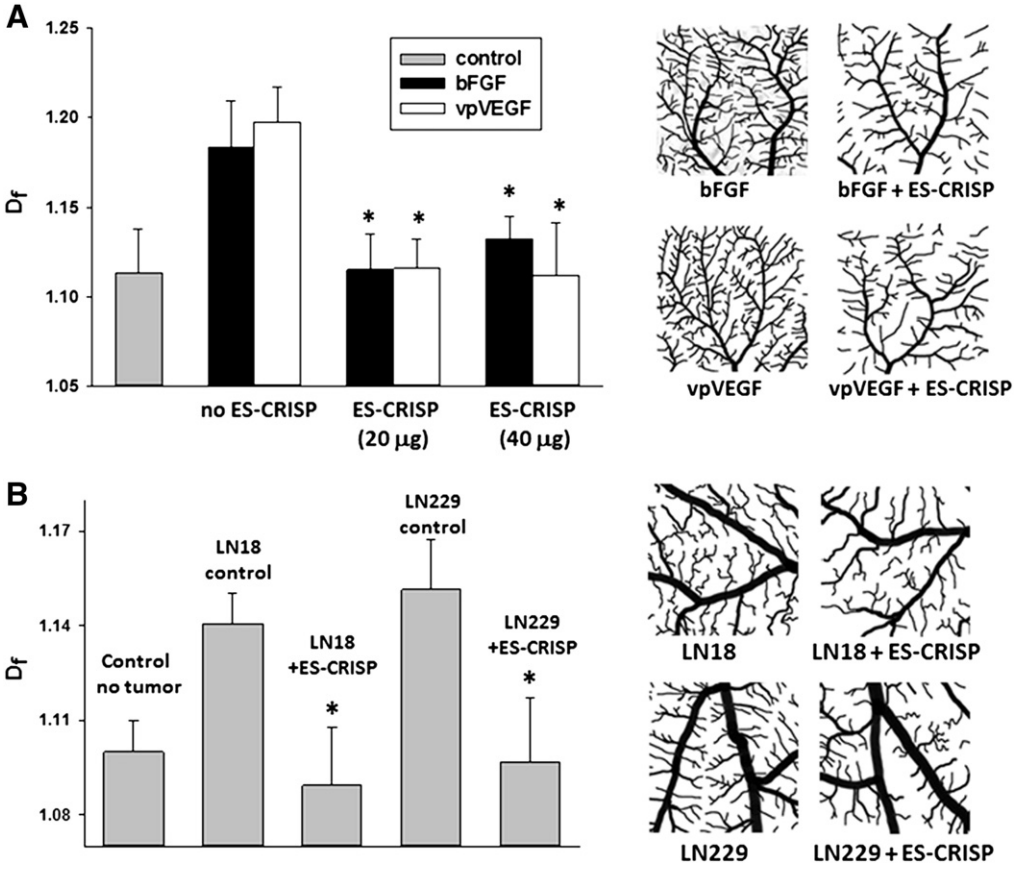

Fig. 6. Effect of ES-CRISP on the angiogenesis, induced in CAM assay of the embryonic quail system. Graphic values of angiogenesis index as a fractal dimension (D_f) are presented on the left plot, representative binary images of analyzed fragments of CAMs dissected from embryos are presented on right panels. (A) Anti-angiogenic effect of ES-CRISP in embryos stimulated by growth factors. Embryos were grown on a 6-well plate until day 7, and treated for 24 h by 0.5 ml volume of PBS in the presence or absence of bFGF (0.5 μg), vpVEGF (0.5 μg) supplemented or not with ES-CRISP (20 or 40 μg). Embryos were fixed, and CAM were dissected and mounted into glass coverslip. The images of CAM were scanned into Photoshop software, mid-arterial endpoints were cropped into ImageJ software, skeletonized and D_f value was calculated. Error bars represent standard deviation from analysis of 5–8 embryos per group. (*) Difference between growth factors treated group ($p < 0.01$). (B) Anti-angiogenic effect of ES-CRISP in embryos with implanted gliomas. Glioma cell lines, LN18 and LN229 were implanted on the CAM in day 7 of embryonic development, and started to treat after 24 h with ES-CRISP (20 μg per 50 μl of PBS). On the embryonic day 13 embryos were fixed, membranes were dissected and angiogenesis was analyzed as described above. (*) Difference between control tumor developing groups and tumor developing groups treated with ES-CRISP ($p < 0.01$).

Table 1
Relative expression of genes encoding factors involved in angiogenesis in ES-CRISP-treated HUVEC.

Gene symbol	Fold change treated/untreated
Down-regulated genes	
ANGPT1	−2.3
CCL2	−2.1
CDH5	−2.0
CTGF	−3.2
EDN1	−4.0
ENG	−2.0
FIGF	−2.5
ITGB3	−2.4
MMP2	−2.0
PGF	−2.4
PTGS1	−2.2
SERPINE1	−3.5
SERPINF1	−2.3
TGFA	−2.8
TGFB2	−8.2
THBS1	−2.9
TIMP2	−2.6
TIMP3	−3.7
Up-regulated genes	
F3	4.5
ID1	3.6
IGF1	3.3
IL8	2.8
MMP9	4.9
PF4	4.4

The genes that were significantly modulated (2-fold up- or down-regulation) are presented. The data demonstrate folds of expression relative to untreated HUVEC cultures.

FAK phosphorylation. On the other hand, two α5β1 integrin ligands, ECM protein fibronectin, and snake venom disintegrin, echistatin very strongly induced autophosphorylation of this focal adhesion kinase (Fig. 7C).

4. Discussion

CRISP proteins have been identified in the majority of eukaryotic organisms, although their functions remain very poorly established. In this article, we report that the snake venom CRISP isolated from *E.c. sochureki* inhibits angiogenesis by direct interaction with endothelial cells. ES-CRISP shares a largely conserved structure with other members of this snake venom protein family. Interestingly, over 50% of the primary structure of ES-CRISP is identical to the human protein, CRISP-3. The physiological relevance of the snake venom CRISP has been studied in the context of its toxicity, which could be important for predation. Indeed, CRISP isolated from various venoms blocks L-type of calcium and cyclic nucleotide gated channels, that may harm the victims [16,17]. However, experimental treatment of mice and insects with these proteins yielded no toxic effects [18]. Our studies with an avian embryonic model confirmed the lack of toxicity of snake venom CRISP, since ES-CRISP in doses up to 40 μg was harmless to quail embryos, which are very sensitive to exogenous toxins. Therefore, it is difficult to classify CRISP as a toxic component of snake venom, unless it interacts synergistically with other venom proteins. High levels of CRISP-3 in human blood appear to confirm this concept, although some reports suggest neutralization of its ion channel-blocking effects by binding to other plasma proteins such as α1B-glycoprotein [21].

The most intriguing observation is that ES-CRISP supports the adhesion of endothelial cells. These cells adhered to the immobilized protein in a dose-dependent manner. We compared adhesion of ES-CRISP to three types of EC in the absence of activating cytokines and found that the binding of cells isolated from glioma tissue was more potent than of those isolated from umbilical cord (HUVEC) or aorta (HAEC). Endothelial cells are activated in cancer tissues as a part of an intensive pro-angiogenic cascade, and the potential receptor for ES-CRISP appears to be up-regulated during this process. Competition experiments with integrin-dependent adhesion of endothelial cells to ECM proteins suggest that ES-CRISP is unable to block the function of this largest family

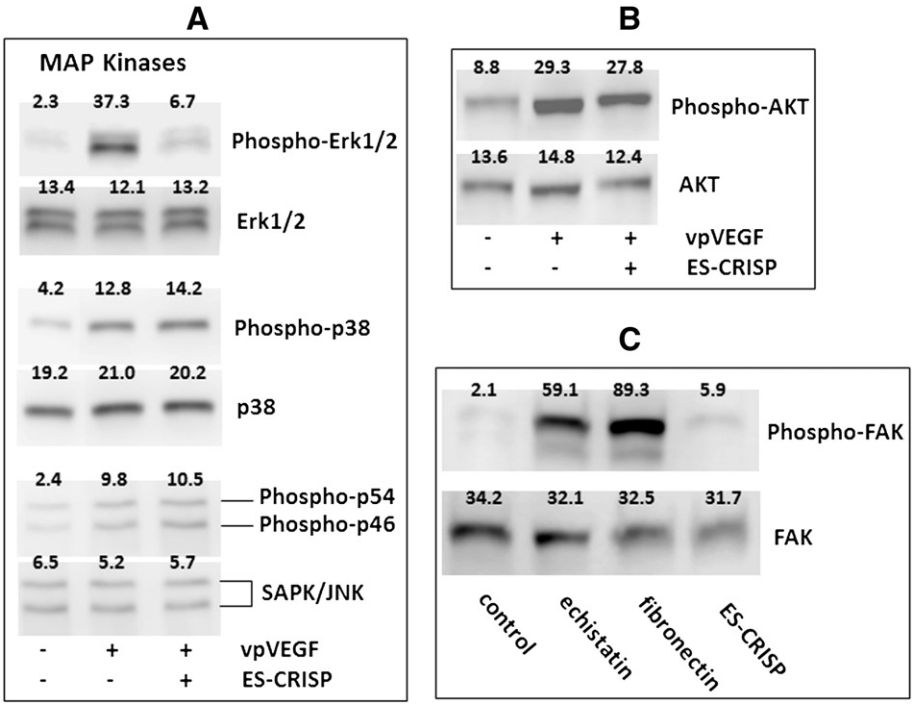

Fig. 7. Effect of ES-CRISP on cell signaling in HUVEC. (A) Effect of ES-CRISP on phosphorylation of MAP kinases induced by vpVEGF. Cells were FBS-starved for 24 h and treated or not with vpVEGF (50 ng/ml) in the presence or absence ES-CRISP (10 μg/ml) for 30 min. Phosphorylation of the proteins was detected using Western blotting as described in Material and methods. (B) Effect of E-CRISP on activation of AKT. Cells were FBS-starved for 24 h and treated or not with vpVEGF and ES-CRISP for 60 min. (C) Effect of ES-CRISP on FAK phosphorylation. Proteins were immobilized on the 6-well plate at conditions as described in Fig. 4. Cells were FBS-starved for 24 h and applied on the wells. After 60 min incubations cells were lysed, and Western blotting was performed as described above. Control was a cell lysate obtained after incubation in bovine serum albumin. The numbers above the bands represent value of average pixels, reflecting intensity of bands, and digitalized using Un-Scan-It software.

of pro-adhesive receptors. Moreover, the majority of cancer cells examined in this study failed to adhere to ES-CRISP, despite that all of these cell lines express a variety of integrins. The only exception was the MV3 human melanoma cell line, which did adhere to ES-CRISP. This observation may be useful for the future identification of the potential CRISP receptor. A high concentration of ES-CRISP is required to promote cell adhesion when compared to typical integrin ligands, such as ECM proteins, or other snake venom proteins, such as disintegrins or CLPs. The morphology of the adhered cells also suggests that supporting adhesion is not a physiological function of ES-CRISP. Cells did not spread on ES-CRISP and remained rounded in shape, in contrast to the integrin-dependent spreading on fibronectin and echistatin.

The attachment-dependent morphological changes of the cell are associated with the generation of cell signaling and focal adhesion plays important role in this process. Therefore, we tested activation of FAK following attachment of HUVEC to the ES-CRISP in comparison to integrin ligands, fibronectin and echistatin. Integrins are the major cellular receptors, which are directly involved in stimulation of FAK for phosphorylation. ES-CRISP showed no activation of FAK suggesting that attachment of cell to this snake venom protein does not induce focal adhesion, and does not generate any integrin-dependent cell signaling in contrast to the typical integrin ligands such as fibronectin and echistatin.

Human CRISP-3 is considered to be a cytokine because it is produced by immune cells such as granulocytes or B-lymphocytes, although its cytokine-related functions were not reported. Cobra venom CRISP affects EC in similar manner to pro-inflammatory cytokines [19]. It increases the expression of adhesion molecules including VCAM-1, ICAM-1 and E-selectins to promote monocyte cell adhesion. On the other hand, ES-CRISP, as shown in this work, reduced the activation of EC resulting in the inhibition of cell proliferation, migration, tube formation, and capillary sprouting that represent all angiogenesis steps. It should be noted that the soluble form of ES-CRISP binds to EC forming clusters on the cell surface and is internalized into the cytoplasm in a granule-like manner. EC express variety of receptors, which may be internalize following to the ligand binding such as integrins [34], receptor tyrosine kinases (growth factor receptors) [35], G-protein coupled receptors [36], and TNF receptors [37]. Therefore, we posit that an as yet unidentified CRISP receptor should be among those, which are involved in endosomal trafficking through the membrane for generation of appropriate cellular response.

In this study, we initiated mechanistic experiments on the effect of ES-CRISP as an anti-angiogenic molecule. Based on distinct pattern of gene expression in HUVEC treated with ES-CRISP, we can distinguish pathways and factors which may be involved in this process. The strongest ES-CRISP-driven down-regulation was observed for transforming growth factor-β (TGF-β), which was previously characterized as a positive angiogenesis regulator in various types of cancer and a promoter of malignancy, especially in the advanced stages [38]. Interestingly TSP-1, which is down-regulated by ES-CRISP, activates TGF-β [39]. TSP-1 is generally considered an inhibitor of angiogenesis; however some studies showed that it may under certain conditions also act as a stimulator of this process, especially at lower concentrations [40]. In support of the latter notion, an N-terminal fragment of TSP-1 has been characterized as pro-angiogenic factor [31]. Therefore, the regulatory effect of ES-CRISP on EC may be a helpful tool to gain a better understanding of the cross-talk between TSP-1 and TGF-β in tumor angiogenesis. Genes up-regulated by ES-CRISP have included anti-angiogenic platelet factor-4 [41], and matrix metalloproteinase-9, which is considered as pro- and anti-angiogenic [42].

ES-CRISP blocked growth factors-induced angiogenesis *in vivo* in quail embryonic CAM assay. Therefore, we investigated effect of ES-CRISP on VEGF-induced activation of typical pro-angiogenic signaling pathways in endothelial cells: MAP kinases that promote cell proliferation and migration, and AKT that supports cell survival by blocking pro-apoptotic molecules. ES-CRISP inhibited MAPK Erk1/2 having no effect on two other MAP kinases, p38 and SAPK/JNK. This observation suggests that VEGF-induced MAPK Erk1/2 pathway may be affected: (i) by cross-talk with cell signaling pathway induced by the hypothetical receptor for ES-CRISP; and (ii) by direct alteration of cell signaling following internalization of ES-CRISP. The internalization of this snake venom protein to the cytoplasm was documented in the presented work. We excluded direct interaction of ES-CRISP with VEGFR and competition with growth factor in this process, because other VEGF-dependent pathways were not affected. Based on these results we can conclude that one of the major mechanisms, which is involved in the blocking of pro-angiogenic activity of endothelial cells, such as proliferation and migration, by ES-CRISP is inhibition of activation of MAPK Erk1/2. Participation of these cell signaling molecules in VEGF-induced angiogenesis is well documented [43].

In summary, we report a new activity of snake the venom CRISP, which may be useful for designing an angiostatic therapy for cancer treatment, as well as for understanding some of mechanisms involved in the angiogenesis-dependent progression of tumor. Since human CRISP-3 molecule shares over 50% identity with ES-CRISP, including a conserved pattern of cysteines, it may also have similar activities, including blocking of angiogenesis. Therefore, circulating in human blood CRISP-3 may be an endogenous negative modulator of angiogenesis. Unbalanced levels of CRISP-3 might participate in cancer progression by turning on the "angiogenic switch". The verification of this hypothesis requires a separate study on human CRISP.

Transparency document

The Transparency document associated with this article can be found, in the online version.

Acknowledgment

The work was supported by grants from the National Cancer Institute NCI R01CA133262 and R01CA100145 (C.M.), and BFU2010-17373 from the Ministerio de Ciencia é Innovación (currently, Ministerio de Economía y Competitividad), Madrid (J.J.C.). PIL is the Laura H. Cornell Professor in the Dept. of Bioengineering, College of Engineering, Temple University. PL holds The Jacob Gitlin Chair in Physiology and is affiliated and partially supported by the Dr. Adolf and Klara Brettler Center for Research in Molecular Pharmacology and Therapeutics at The Hebrew University of Jerusalem and Israel Science Foundation, Israel

Appendix A. Supplementary data

Supplementary data to this article can be found online at http://dx.doi.org/10.1016/j.bbagen.2015.02.002.

References

[1] J. Folkman, Tumor angiogenesis: therapeutic implications, N. Engl. J. Med. 285 (1971) 1182–1186.
[2] D. Carpizo, M.L. Iruela-Arispe, Endogenous regulators of angiogenesis—emphasis on proteins with thrombospondin-type I motifs, Cancer Matastasis Rev. 19 (2000) 159–165.
[3] D. Hanahan, J. Folkman, Patterns and emerging mechanisms of the angiogenic switch during tumorigenesis, Cell 86 (1996) 353–364.
[4] L. Amit, I. Ben-Aharon, L. Vidal, L. Leibovici, S. Stemmer, The impact of Bevacizumab (Avastin) on survival in metastatic solid tumors—a meta-analysis and systematic review, PLoS One 8 (2013) e51780.
[5] C. Marcinkiewicz, Applications of snake venom components to modulate integrin activities in cell–matrix interactions, Int. J. Biochem. Cell Biol. 45 (2013) 1974–1986.
[6] M.A. McLane, T. Joerger, A. Mahmoud, Disintegrins in health and disease, Front. Biosci. 13 (2008) 6617–6637.
[7] E.M. Walsh, C. Marcinkiewicz, Non-RGD-containing snake venom disintegrins, functional and structural relations, Toxicon 58 (2011) 355–362.
[8] T. Momic, G. Cohen, R. Reich, F.T. Arlinghaus, J.A. Eble, C. Marcinkiewicz, P. Lazarovici, Vixa-patin (VP12), a C-type lectin-protein from Vipera xantina palestinae venom:characterization as a novel anti-angiogenic compound, Toxins (Basel) 4 (2012) 862–877.

[9] C. Chung, W. Wu, T. Huang, Aggretin, a snake venom–derived endothelial integrin α2β1 agonist, induces angiogenesis via expression of vascular endothelial growth factor, Blood 103 (2004) 2105–2113.
[10] R. Zouari-Kessentini, N. Srairi-Abid, A. Bazaa, M. El Ayeb, J. Luis, N. Marrakchi, Anti-tumoral potential of Tunisian snake venoms secreted phospholipases A2, Biomed. Res. Int. (2013) 391389.
[11] J.M. Gutiérrez, B. Lomonte, L. Sanz, J.J. Calvete, D. Pla, Immunological profile of antivenoms: preclinical analysis of the efficacy of a polyspecific antivenom through antivenomics and neutralization assay, J. Proteomics 105C (2014) 340–350.
[12] A.S. Ramazanova, V.G. Starkov, A.V. Osipov, R.H. Ziganshin, S.Y. Filkin, V.I. Tsetlin, Y.N. Utkin, Cysteine-rich venom proteins from the snakes of Viperinae subfamily—molecular cloning and phylogenetic relationship, Toxicon 53 (2009) 162–168.
[13] Y. Shikamoto, K. Suto, Y. Yamazaki, T. Morita, H. Mizuno, Crystal structure of a CRISP family Ca^{2+}-channel blocker derived from snake venom, J. Mol. Biol. 350 (2005) 735–743.
[14] X. Tu, J. Wang, M. Guo, D. Zheng, M. Teng, L. Niu, et al., Purification, partial characterization, crystallization and preliminary X-ray diffraction of two cysteine-rich secretory proteins from *Naja atra* and *Trimeresurus stejnegeri* venoms, Acta Crystallogr. D60 (2004) 1108–1111.
[15] Y. Yamazaki, T. Morita, Structure and function of snake venom cysteine-rich secretory proteins, Toxicon 44 (2004) 227–231.
[16] Y. Yamazaki, H. Koike, Y. Sugiyama, K. Motoyoshi, T. Wada, S. Hishinuma, M. Mita, T. Morita, Cloning and characterization of novel snake venom proteins that block smooth muscle contraction, Eur. J. Biochem. 269 (2002) 2708–2715.
[17] R.L. Brown, T.L. Haley, K.A. West, J.W. Crabb, Pseudechetoxin: a peptide blocker of cyclic nucleotide-gated ion channels, Proc. Natl. Acad. Sci. U. S. A. 96 (1999) 754–759.
[18] Y.N. Utkin, A.V. Osipow, Non-lethal polypeptide components in Cobra venom, Curr. Pharm. Des. 13 (2007) 2906–29015.
[19] Y.L. Wang, J.H. Kuo, S.C. Lee, J.S. Liu, Y.C. Hsieh, Y.T. Shih, C.J. Chen, J.J. Chiu, W.G. Wu, Cobra CRISP functions as an inflammatory modulator via a novel Zn^{2+}- and heparan sulfate-dependent transcriptional regulation of endothelial cell adhesion molecules, J. Biol. Chem. 285 (2010) 37827–37883.
[20] L. Udby, J.B. Cowland, A.H. Johnsen, O.E. Sørensen, N. Borregaard, L. Kjeldsen, An ELISA for SGP28/CRISP-3, a cysteine-rich secretory protein in human neutrophils, plasma, and exocrine secretions, J. Immunol. Methods 263 (2002) 43–55.
[21] L. Udby, O.E. Sorensen, J. Pass, A.H. Johnsen, N. Borregaard, L. Kjeldsen, Cysteine-rich secretory protein 3 is a ligand of alpha1B-glycoprotein in human plasma, Biochemistry 43 (2004) 12877–12886.
[22] A.A. Breed, A. Gomes, B.S. Roy, S.D. Mahale, B.R. Pathak, Mapping of the binding sites involved in PSP94–CRISP-3 interaction by molecular dissection of the complex, Biochim. Biophys. Acta 1830 (2013) 3019–3029.
[23] A. Bjartell, R. Johansson, T. Bjork, V. Gadaleanu, A. Lundwall, H. Lija, L. Kjeldsen, L. Udby, Immunohistochemical detection of cysteine-rich secretory protein 3 in tissue and in serum from men with cancer or benign enlargement of the prostate gland, Prostate 66 (2006) 591–603.
[24] H. Ye, T. Yu, S. Temam, B.L. Ziober, J. Wang, J.L. Schwartz, L. Mao, D.T. Wong, X. Zhou, Transcriptomic dissection of tongue squamous cell carcinoma, BMC Genomics 9 (2008) 69.
[25] P. Jakubowski, J.J. Calvete, J.A. Eble, P. Lazarovici, C. Marcinkiewicz, Identification of C-lectin type proteins in *Echis suchoreki* venom, which interact with α2β1 integrin, Toxicol. Appl. Pharmacol. 269 (2013) 34–42.
[26] S. Bazan-Socha, D.G. Kisiel, B. Young, R.D.G. Theakston, J.J. Calvete, D. Sheppard, C. Marcinkiewicz, Structural requirements of MLD-containing disintegrins for functional interaction with α4β1 and α9β1 integrins, Biochemistry 43 (2004) 1639–1647.
[27] N.R. Casewell, R.A. Harrison, W. Wüster, S.C. Wagstaff, Comparative venom gland transcriptome surveys of the saw-scaled vipers (Viperidae: *Echis*) reveal substantial intra-family gene diversity and novel venom transcripts, BMC Genomics 10 (2009) 564.
[28] C. Marcinkiewicz, L.A. Rosenthal, D.M. Mosser, T.J. Kunicki, S. Niewiarowski, Immunological characterization of eristostatin and echistatin binding sites on αIIbβ3 and αvβ3 integrins, Biochem. J. 317 (1996) 817–825.
[29] M.C. Brown, J.J. Calvete, I. Staniszewska, L. Del Valle, P. Lazarovici, C. Marcinkiewicz, VEGF-related protein isolated from *Vipera palestinae* venom, promotes angiogenesis, Growth Factors 25 (2007) 108–117.
[30] E.M. Walsh, R. Kim, M. Weaver, L. Del Valle, J. Sheffield, P. Lazarovici, C. Marcinkiewicz, Importance of interaction of NGF with α9β1 integrin in progression of glioma angiogenesis, Neuro-Oncol. 14 (2012) 890–901.
[31] I. Staniszewska, S. Zaveri, L. Del Valle, I. Oliva, V.L. Rothman, S.E. Croul, D.D. Roberts, D.F. Mosher, G.P. Tuszynski, C. Marcinkiewicz, Interaction of α9β1 integrin with thrombospondin-1 promotes angiogenesis, Circ. Res. 100 (2007) 1308–1316.
[32] S. Lecht, J.A. Gerstenhaber, C.T. Stabler, P. Pimton, S. Karamil, C. Marcinkiewicz, E.S. Schulman, P.I. Lelkes, Heterogeneous mixed-lineage differentiation of mouse embryonic stem cells induced by conditioned media from A549 cells, Stem Cells Dev. 23 (2014) 1923–1936.
[33] K. Meerovitch, F. Bergeron, L. Leblond, B. Grouix, C. Poirier, M. Bubenik, et al., A novel RGD antagonist that targets both alphavbeta3 and alpha5beta1 induces apoptosis of angiogenic endothelial cells on type I collagen, Vasc. Pharmacol. 40 (2003) 77–89.
[34] M.R. Morgan, A. Byron, M.J. Humphries, M.D. Bass, Giving off mixed signals—distinct functions of α5β1 and αvβ3 integrins in regulating cell behavior, IUBMB Life 61 (2009) 731–738.
[35] A. Eichmann, M. Simons, VEGF signaling inside vascular endothelial cells and beyond, Curr. Opin. Cell Biol. 24 (2012) 188–193.
[36] A. Marchese, Endocytic trafficking of chemokine receptors, Curr. Opin. Cell Biol. 27 (2014) 72–77.
[37] M.E. Guicciardi, G.J. Gores, Life and death by death receptors, FASEB J. 23 (2009) 1625–1637.
[38] E.F. Saunier, R.J. Akhurst, TGF beta inhibition for cancer therapy, Curr. Cancer Drug Targets 6 (2006) 565–578.
[39] S.E. Crawford, V. Stellmach, J.E. Murphy-Ullrich, S.M. Ribeiro, J. Lawler, R.O. Hynes, G.P. Boivin, N. Bouck, Thrombospondin-1 is a major activator of TGF-β1 in vivo, Cell 93 (1998) 1159–1170.
[40] X. Qian, T.N. Wang, V.L. Rothman, R.F. Nicosia, G.P. Tuszynski, Thrombospondin-1 modulates angiogenesis in vivo by up-regulation of matrix metalloproteinase-9 in endothelial cells, Exp. Cell Res. 235 (1997) 403–412.
[41] A. Bikfalvi, Platelet factor 4: an inhibitor of angiogenesis, Semin. Thromb. Hemost. 30 (2004) 379–385.
[42] A. Pozzi, P.E. Moberg, L.A. Miles, L.A. Wagner, P. Soloway, H.A. Gardner, Elevated matrix metalloprotease and angiostatin levels in integrin alpha 1 knockout mice cause reduced tumor vascularization, Proc. Natl. Acad. Sci. U. S. A. 97 (2000) 2202–2207.
[43] L. Claesson-Welsh, M. Welsh, VEGFA and tumour angiogenesis, J. Intern. Med. 273 (2013) 114–127.
[44] J. Kratzschmar, B. Haendler, U. Eberspaecher, D. Roosterman, P. Donner, W.D. Schleuning, The human cysteine-rich secretory protein (CRISP) family, Primary structure and tissue distribution of CRISP-1, CRISP-2 and CRISP-3, Eur. J. Biochem. 236 (1996) 827–836.